Micro-magnetic resonance imaging (μ-MRI) study on the sepsis effected eyeball of zebrafish

Bimal Kumar Sarkar[1], Wu Zen[1], Shangwu Ding[1], C. H. Hsu[2], Z.H. Wen[2], C. S. Lin[2] and Chiranjib Chakraborty[2*]

[1] *Department of Chemistry, National Sun Yat-sen University, Kaohsiung, Taiwan 80424*

[2] *Department of Marine Biotechnology and Resources; College of Marine Science; National Sun Yat-sen University; Kaohisung; Taiwan 80424*

*Corresponding author. *Fax :* +886-07-5252011

E-mail address. drchiranjib@yahoo.com

Abstract

We have studied the normal and sepsis effected zebrafish eyeball with micro-magnetic resonance imaging (micro-MRI). T_2 weighted image was studied and pixel-wise T_2 maps were co registered among the normal and sepsis effected eye. From the micro-image the sepsis effect in the eye has been demonstrated. The pixel-wise brightness distribution is not so scattered in the normal eyeball image, whereas it is very scattered in case of sepsis affected eyeball image. Also the T_2 mapping on the eye has given valuable information that would be a potential tool for the study of diseased organ in the micro level. From T_2 mapping, it has shown that the T2 in normal eyeball have low values in comparison to the sepsis affected eyeball.

Keywords: Zebrafish; Eyeball; Micro-Magnetic Resonance Imaging; T_2 weighted image; T_2-map.

Introduction

The zebrafish, one of the favourite animals of developmental biologists, is rapidly gaining ground in infection models [1,2]. With the zebrafish, genetic screens in a vertebrate host with a fully developed immune system are possible [3,4]. In addition, bacterial infections can be analyzed in real-time in zebrafish embryos [5]. This fish is a unique and important animal model in which the power of mutagenesis is applied to the study of vertebrate development [6,7]. Zebrafish genome mutagenesis has provided important insights into genes related to cardiac, vascular, and erythrocyte development, including models of disease such as congenital sideroblastic anemia and hepatoerythropoietic porphyria [6-9]. Given the development of appropriate screening assays, the power of the zebrafish model can be harnessed for the study of other vertebrate functions such as hemostasis, thrombosis and sepsis [10-13]. Previous research with zebrafish ensured that a variety of human disease conditions are can be studied utilizing the zebrafish model [14,15].

It is well known that T_2 plays a role in almost every aspect of nuclear magnetic resonance [16]. Clinical T_2-weighted images were exquisitely sensitive to neuro pathology, giving rise to much optimism that T_2 relaxation would lead to pathological specificity [17]. T_2 relaxation rates can be correlated to the pathological changes observed in neurodegenerative diseases including edema (increased intra- or extracellular water), blood–brain barrier collapse (tight junction leakage), inflammation (proliferation of inflammatory cells), demyelination (breakdown of the myelin sheath), gliosis

(proliferation of glial cells) and axonal loss (breakdown ofthe axon) [18]. The level to which these pathologies can be measured by MRI depends upon whether they have a unique impact on the proton NMR signal; if these pathological changes affect the organisation of nonaqueous molecules in cellular structures, water T_2 relaxation should also be affected. The features allied with pressure ulcers that may affect muscle proton density and relaxation times are inflammation, edema, necrosis, hemorrhage, fibrosis, and fatty infiltration[19-21]. These diseases like inflammation, edema, and also hemorrhage can lead to an increased proton density which is caused by an increased in both intracellular and extracellular free water. T_2 is very sensitive to tissue changes [22] which were noted in animal model Brown-Norway rats where tibialis anterior (TA) was condensed by means of an indenter. After 24 h, muscle tissue variation was observed by using MRI. It was shown that affected tissue localized by T_2-weighted MRI correlated well with damaged areas determined by histological examination. A raise in the transverse relaxation time (T_2) is generally established as a measurement of tissue injury [23].

However, there no previous report to study the zebrafish diseases model using MRI. So, it is very relevant to study the sepsis model using MRI. Here we have investigated the sepsis induced eyeball of zebrafish (*Danio rerio*) by MR micro-imaging giving special emphasis on the transverse relaxation mapping and we took an opportunity also to shed

light on micro-level for the study of sepsis effect on the eyeball with the help of micro-MRI.

Materials and methods

Zebrafish model. Adult zebrafish were obtained from the lab stock maintained according to the guidelines given in the zebrafish book [24]. The fish used in these experiments were about 4-6 months old and approximately 3 cm in length which were kept in 5-10 lit glass aquariums. The aquaria had a continuous re-circulating system, consisting of biological filters. Additional oxygen was provided by placing air-stones in the water and 1/3 of water was replaced weekly. Aquariums water temperature was maintained at 28.5°C-32°C and a constant 14/10-h light/dark cycle.

Sepsis effected zebrafish. All zebrafish were injected at the age of 4-6 months old. BD ultra-fine II insulin syringe (1-2 cc capacity) was used for injection (Becton Dickinson). Fishes were admitted to the study ward at 8:00 am after an overnight fast. The volume of injection was maintained constant at 10 µl, and the amount of LPS was 2 ng/kg LPS (Sigma, USA). The fishes were taken out of the water and provided anesthesia with MS-222 (a methane sulfonate salt of 3-aminobenzoic acid ethyl ester, Sigma Chemical Company, St. Louis, MO, USA) at a concentration of 50 mg/100 ml for 5-10 minutes and then an intra-muscular injection was given approximately in the end region

of the dorsal fin on one flank of the fish. Identical volumes of saline were given in the control group.

Collection of samples. We have operated and collected zebrafish's eyeball for (1) normal and (2) sepsis affected, very carefully to collect the eyeball. The eye was kept in liquid nitrogen for quick freezing. Within 24 hours we have used the sample for study.

Micro-imaging. All MR images of the zebrafish eyeball were obtained with a Varian Unity INOVA 500 MHz NMR spectrometer with 11.4 Tesla magnetic fields in vertical bore Oxford 500 magnet system at a 500-MHz proton Larmor frequency. The system was interfaced to a Linux PC running Solaris 9 operating environment on Sun SPARC host workstation. T_2-weighted images [25] were acquired using spin echo multi scan (SEMS) pulse sequence. Subsequent T_2- weighted images were acquired using multiple echo time (TE). The MR parameters were: repetition time (TR) = 1000 msec (90° flip angle), effective echo time (TE) = 12, 16, 20, and 25 msec, spectral width = 50 kHz, 8 averages, field of view (FOV) = 0.3 cm × 0.3 cm, data matrix = 128 × 128, and number of transients (NT) = 32.

Data Analysis. T_2 have been calculated pixel-by-pixel of the region of interest (ROI) according to the relation,

$$S(TE) = S_0 g \exp(-TE / T_2) \qquad \ldots(1)$$

where TE is the effective echo time at the center of the echo-train length, and S_0 is the signal intensity at TE = 0. T_2 were derived using nonlinear least squared regression with Mathematica 5.0. In the regression process, for each pixel, we have taken the signal intensity for different TE values. Thus we can find the T_2 values for each pixel.

Results

The zebrafish eyeball, one is normal and other as sepsis effected, were used to collect micro-MR images with three different TE weightings (TE = 12, 16 and 20 ms). We have taken dorsal -median plane section of the eyeball (Fig. 1D). The FOV was 0.3 × 0.3 cm^2. Nearly uniform brightness appeared in different parts of the normal eyeball (Fig. 1 A, B and C). Also the images for sepsis affected eye are shown in Fig. 2 A, B and C. The histograms of the pixel-wise brightness distribution in the image with TE=12 ms for normal and sepsis effected eyes are shown respectively in Fig. 3 A and B. It is understood from the histogram for the normal eye that more or less the pixels are around the intensity value 0.0002 (in arbitrary unit) with median 0.0002307 and standard deviation 0.0001684 (Table 1). We have considered total 6717 pixels in the image. But there is remarkable variation in brightness in the different parts in T_2-weighted image of the sepsis affected eyeball (Fig. 2 A, B and C). The histogram of the pixel-wise

brightness distribution of the sepsis effected eye shows that the distribution is scattered with median 0.0006318 and standard deviation 0.0003504 (Table 1).

For precise understanding, a ROI was taken just in the backside of the lens in between the lens and the retina (Fig. 2 D). We have taken the ROI both for normal and sepsis effected eye for comparison. The histograms of the pixel-wise brightness distribution in the ROIs are depicted in Fig. 3, C and D for normal and sepsis affected eye respectively. The histogram shows for the normal eye that the pixels are around the intensity value 0.0009 (in arbitrary unit) with median 0.0009154 and standard deviation 0.0001451 (Table 2). For sepsis effected ROI, the distribution is comparatively more scattered with median 0.00113 and standard deviation 0.0001253 (Table 2).

T2 have been calculated pixel-by-pixel as explained in the data analysis section. The T_2 mappings for normal eye and the sepsis affected one are shown in Fig 4 A and B. The mapping indicates that T_2 have greater values in case of sepsis affected eye. Most of the part in the sepsis affected one is characterized with T_2 values greater than 200 ms. But in the normal eye, T_2 values are in the range from 75 ms to 200 ms.

Discussion

The major findings of this study are: (1) T_2-weighted images and (2) T_2 mapping of normal and sepsis effected eye of zebrafish. From T_2-weighted images, it is found that there is a more variation in the brightness in sepsis effected eyeball image. But there is

not so much variation in the normal eyeball image. Also it is clear from the histogram that the pixel-wise brightness distribution is not so scattered in the normal eyeball, whereas it is very scattered in case of sepsis effected eyeball. From T_2 mapping, it is shown that the T_2 in normal eyeball have comparatively low values. But the T_2 have the larger values in sepsis affected eyeball. It can be understood from the T_2 weighted anatomical and T_2 mapping images, that T_2 is very sensitive to the pathological change in tissues. The relaxation properties of water, which may be characterized by a longitudinal or spin-lattice relaxation time T_1 and a transverse or spin-spin relaxation time T_2, play a crucial role [26]. These values depend in a characteristic way on molecular environment of water molecules, because of different molecular mobility and structures. Also, water protons can exchange themselves or the magnetization with mobile protons of external functional OH- or NH-groups of the proteins leading also to contributions of these environments to water relaxation times [27,28]. Nevertheless, these quantities can provide interesting information on changes of protein hydration and mobility, which are themselves related to biological changes [29,30]. The spin-spin relaxation time T_2 is a specific attribute of spins that depends on their surroundings. Interaction between spins (e.g., coupling of neighboring nuclei) destroys the phase coherence, and therefore the T_2 relaxation time can be a sensitive indicator of impaired cell physiology. In the sepsis effected region on the eyeball, it causes the ingression of intracellular and extracellular free water which in turn results in an increase in T_1 (longitudinal relaxation time) and T_2.

T_2 is very sensitive to tissue changes. An increase in the transverse relaxation time (T_2) is an expression of tissue damage.

However, MRI can measure structural, physiological (like blood flow and oxygenation) and, metabolic data in a single setting, which are generally not possible with present techniques and that is the great advantage of MRI. It has no depth limitation also. Therefore, MRI has the potential to complement existing techniques to study the eyeball.

In conclusion, the pathological changes due to the sepsis in the zebrafish eyeball were resolved using multiple MRI contrasts. To the best of our knowledge, this is the first micro-MRI study in demonstrating the damage in the sepsis affected eyeball of zebrafish. Further improvements are expected for this model. MRI has the potential to provide sepsis affected physiological (such as tissue blood flow and oxygenation) and functional information on the organ of micro-dimension in a single setting without depth limitation and, thus, it could complement existing techniques to study very small size organ.

Acknowledgments

This work is particularly supported by "Aim for the Top University Plan" of the National Sun Yat-sen University and Ministry of Education, Taiwan. And project grant NSC 94-2113-M-110-013 from NSC , Taiwan, R.O.C.

References

[1] M. N. Neely, J. D. Pfeifer, M. Caparon, Streptococcus-zebrafish model of bacterial pathogenesis, Infection and Immunity 70 (2002) 3904-3914.

[2] J. D. Miller, M. N. Neely, Zebrafish as a model host for streptococcal pathogenesis, Acta Tropica 91 (2004) 53-68.

[3] J. H. Postlethwait, Y. L. Yan, M. A. Gates, S. Horne, A. Amores, A. Brownlie, A. Donovan, E. S. Egan, A. Force, Z. Gong, C. Goutel, A. Fritz, R. E. Kelsh, E. Knapik, B. Liao, D. Paw, A. Ransom, M. Singer, T. S. Thomson, P. Abduljabbar, D. Yelick, J. Beier, S. Joly, D. Larhammar, F. Rosa, Vertebrate genome evolution and the zebrafish gene map, Nat. Genet. 18 (1998) 345-349.

[4] N. S. Trede, A. G. Zapata, L. I. Zon, Fishing for lymphoid genes, Trends Immunol. 22 (2001) 302-307.

[5] C.S. Lam, V. Korzh, U. Strähle, Zebrafish embryos are susceptible to the dopaminergic neurotoxin MPTP, Eur. J. Neurosci. 21 (2005) 1758-62.

[6] W. Driever, M. C. Fishman, The zebrafish: heritable disorders in transparent embryos, J Clin Invest 97 (1996) 1788 – 1794.

[7] S. H. Orkin, L.I. Zon, Genetics of erythropoiesis:induced mutations in mice and zebrafish, Annu. Rev. Genet. 31 (1997) 33 – 60.

[8] A. Brownlie, A. Donovan, S.J. Pratt, Positional cloning of the zebrafish sauternes gene: a model for congenital sideroblastic anaemia, Nature Genet. 20 (1998) 244 – 250.

[9] H. Wang, Q. Long, S.D. Marty, S. Sassa, S. Lin, A zebrafish model for hepatoerythropoietic porphyria, Nature Genet. 20 (1998) 239 – 243.

[10] P. Jagadeeswaran, Y. Liu, A hemophilia model in zebrafish: analysis of hemostasis, Blood Cells Mol. Dis. 23 (1997) 52 – 57.

[11] P. Jagadeeswaran, Y. Liu, Developmental expression of thrombin in zebrafish embryos: a novel model to study hemostasis, Blood Cells Mol. Dis. 23 (1997) 147 – 156.

[12] P. Jagadeeswaran, Y. Liu, ehan JP She, Analysis of hemostasis in zebrafish, Methods Cell Biol. 59 (1999) 337 – 357.

[13] P. Jagadeeswaran, Zebrafish: a tool to study hemostasis and thrombosis, Curr Opin Hematol. 12 (2005) 149 - 52.

[14] B. A. Barut, L.I. Zon, Realizing the potential of zebrafish as a model for human disease, Physiol. Genomic 2 (2000) 49-51.

[15] P. Alestrom, J. L. Holter, R. Nourizadeh-Lillabadi, Zebrafish in functional genomics and aquatic biomedicine, Trends Biotechnol. 24 (2006) 15-21.

[16] M. Mehring, Principles of High Resolution NMR in solids, 2nd ed., Springer-Verlag, NY, 1983.

[17] H. W. Fischer, P. A. Rinck, Haverbeke Y. Van, R. N. Muller, Nuclear relaxation of human brain gray and white matter: analysis of field dependence and implications for MRI, Magn. Reson. Med. 16 (1990) 317–34.

[18] D. Zhao, L. Jiang, E. W. Hahn, R. P. Ason, Continuous low-dose (metronomic) chemotherapy on rat prostate tumors evaluated using MRI in vivo and comparison with histology, Neoplasia 7 (2005) 678 – 687.

[19] T. Husain, An experimental study of some pressure effects on tissues, with reference to the bed-sore problem, J. Pathol. Bacteriol. 66 (1953) 347–358.

[20] M. Kosiak, Etiology of decubitus ulcers, Arch. Phys. Med. Rehabil. 42 (1961) 19–29.

[21] J.F. Vleet, V.J. Ferrans, Pathological reaction of skeletal muscle to injury, in: T. C. Jones, U. Mohr, R. D. Hunt (Eds.), Cardiovascular and Musculoskeletal Systems: Monographs in Pathology of Laboratory Animals, New York, Springer-Verlag, 1991 pp. 109–126.

[22] E.M.H. Bosboom, C.V.C. Bouten, C.W.J. Oomens, S. H.W.M. Van, F.P.T. Baaijens, H. Kuipers, Quantification and localisation of damage in rat muscles after

controlled loading: a new approach to study the aetiology of pressure sores, Med. Eng. Phys. 23 (2001) 195–200.

[23] J.L. Fleckenstein, Skeletal muscle evaluated by MRI, In: DM Grant and RK Harris (Eds.), Encyclopedia of Nuclear Magnetic Resonance, Chichester, UK, Wiley, 1996, pp. 4430–4436.

[24] M. Westerfield, The zebrafish book: a guide for the laboratory use of zebrafish, (Brachydanio rerio), University of Oregon Press, Eugene, 2nd edition. 1995.

[25] Q. Shen, H. Cheng, M. T. Pardue, T. F. Chang, G. Nair, V.T. Vo, R. D. Shonat, T. Q. Duong, Magnetic resonance imaging of tissue and vascular layers in the cat retina, J. Mag. Reso. Imag. 23 (2006) 465–472.

[26] J.M. Hutchison, NMR proton imaging. in: M.-A. Foster (Ed.), Magnetic Resonance in Medicine and Biology, Pergamon Press, Oxford, pp. 157-212, 1985.

[27] H.T.Edzes, E.T. Samulski, Cross-relaxation and spin diffusion in proton NMR of hydrated collagen, Nature 265 (1977) 259-262.

[28] S.H. Koenig, R.G. Bryant, K. Hallenga,, G.S. Jacob, Magnetic cross-relaxation among protons in protein solutions, Biochemistry 17 (1978) 4348-4358.

[29] P.T. Beall, S.R. Amtey, S.R. Kasturi, NMR Data Handbook for Biomedical Applications, Pergamon Press, New York, 1984.

[30] P. A. Bottomley, T.H. Foster, R.E. Argersinger, L.M. Pfcifcr, A review of normal tissue hydrogen NMR relaxation times and relaxation mechanisms from 1 - 100

MHz: dependence on tissue type, NMR frequencies, temperature, species, excision, and age, Med. Phys. 11 (1984) 425-447.

Table 1

Histogram of the pixel wise intensity distribution in the eyeball.

Eyeball	Number of Pixels/Area	Minimum intensity (arbitrary unit)	Maximum intensity (arbitrary unit)	Median	Mean	Standard Deviation
Normal	6717/0.0369	4.719e-06	0.0008	0.0002307	0.0002737	0.0001684
Sepsis effected	6971/0.03829	2.14e-06	0.0014	0.0006318	0.0006544	0.0003504

Table 2

Histogram of the pixel wise intensity distribution in the ROI.

ROI	Number of Pixels/Area	Minimum intensity (arbitrary unit)	Maximum intensity (arbitrary unit)	Median	Mean	Standard Deviation
Normal	1673/0.00919	0.000391 8	0.001257	0.000915 4	0.000890 1	0.000145 1
Sepsis effected	1353/ 0.007432	0.000722 6	0.001484	0.00113	0.001128	0.000125 3

Figure captions

Fig. 1. T_2 weighted Micro-MR images of normal zebrafish eye with TE (A) 12, (B) 16 and (C) 20 ms and (D) schematic dorsal -median plane section.

Fig. 2. T_2 weighted Micro-MR images for sepsis effected zebrafish eye with TE (A) 12, (B) 16 and (C) 20 ms and (D) ROI in the backside of the lens in between the lens and the retina (indicated as dotted line loop) in the normal eye.

Fig. 3. The histograms of the pixel-wise brightness distribution in the image with TE=12 ms for (A) normal and (B) sepsis effected eyes (C) the ROI in Normal (D) the ROI in sepsis effected eye.

Fig. 4. The T_2 mappings for normal and the sepsis effected eye. (T_2 values are indicated as black colour code)

Fig. 1.

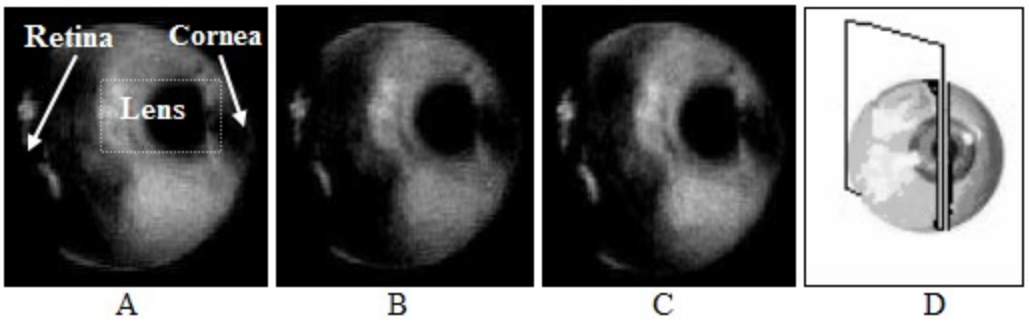

Fig. 2.

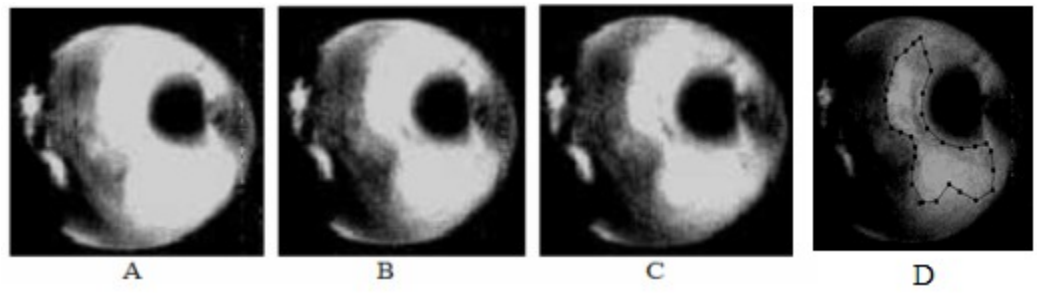

Fig. 3.

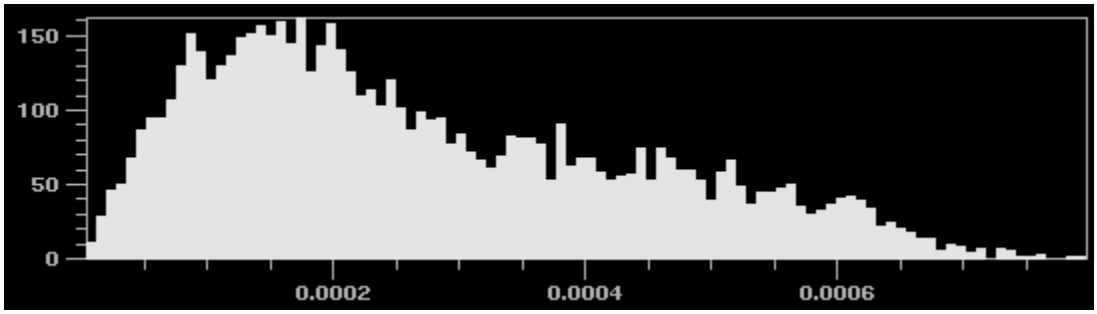

A

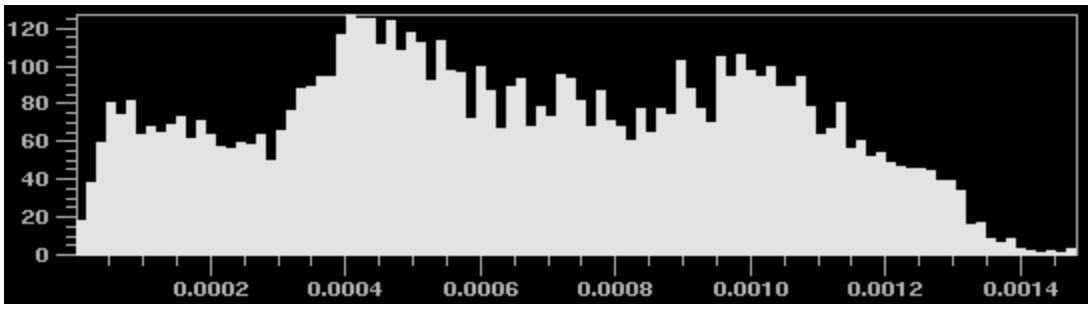

B

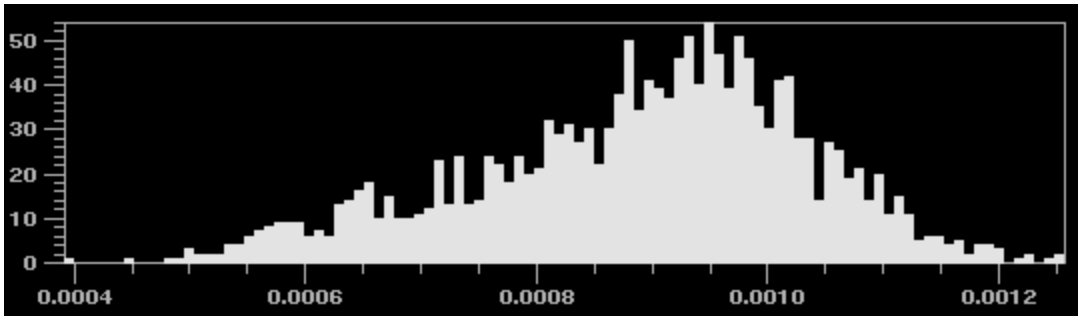

C

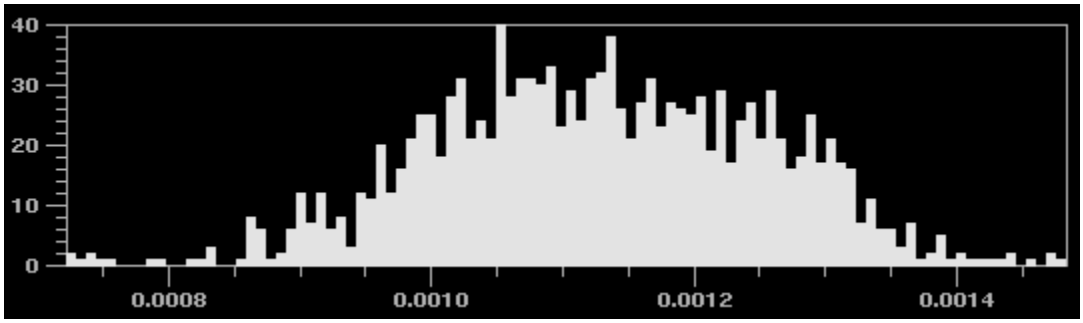

D

Fig. 4.

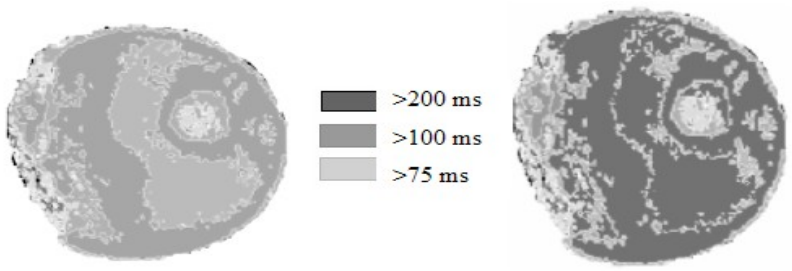

A B